



Characterization of $\text{MmNi}_{3.6}\text{Co}_{0.75}\text{Mn}_{0.55}\text{Al}_{0.1}$ alloys prepared by casting and quenching techniques

Chuanjian Li^{*}, Xinlin Wang, Chongyu Wang

Advanced Materials Institute, Central Iron and Steel Research Institute, Beijing 100081, China

Received 1 August 1997; accepted 6 December 1997

Abstract

An investigation is made of the effects of the solidification rate on the electrochemical properties and structure of alloys with composition $\text{MmNi}_{3.6}\text{Co}_{0.75}\text{Mn}_{0.55}\text{Al}_{0.1}$. By using the rapid quenching preparation technique, the electrode durability of this hydride-forming compound can be greatly improved at the expense of a small decrease in capacity compared with those of the cast alloy. Rapid quenching can also flatten and raise the discharge voltage plateau to a much more promising level, but rapidly quenched alloys generally show a lower activation speed. The higher the quenching rate, the longer the cycle life, the higher and flatter the discharge voltage plateau, but the lower the capacity. X-ray diffraction patterns and SEM observations indicated that whereas there are segregations in the master alloy, there are none in as-quenched alloys whose crystal grain is much smaller than that of the master alloy. © 1998 Elsevier Science S.A. All rights reserved.

Keywords: Hydrogen-storage alloy; Cast; Quench; Electrochemical property; Phase

1. Introduction

The use of metal hydrides as electrodes in rechargeable batteries was first proposed by Justi et al. [1] in 1970. LaNi_5 has been the most promising material for this application because it allows the rapid and reversible storage of large quantities of hydrogen ($\text{H}/\text{M} \approx 1$). The storage capacity of the LaNi_5 electrode declines drastically, however, during repeated charge–discharge cycles (i.e., 50% loss of capacity in 100 cycles). According to Willems [2], this decline is due to the rapid pulverization of the alloy. The pulverization is ascribed to a lattice expansion of about 25 vol% during cycling which leads to huge mechanical tensions in the material. Willems [2] reported in 1984 that the long-term stability of electrodes made of LaNi_5 can be improved by the addition of other alloying elements, especially Co. Cobalt appears to be indispensable in commercial alloys, because with only a partial substitution of nickel by cobalt, the cycling stability

can be improved to a competitive level compared with other types of battery. Unfortunately, cobalt can also decrease the capacity at high discharge current densities. Moreover, cobalt is an expensive metal and this results in a sharp rise in raw material costs. Later, a breakthrough was made which has resulted in multi-component alloys being employed nowadays [3,4].

With replacement of Mischmetal (Mm) for La, Mm-based hydrogen-storage alloys are very useful and low-cost negative electrode materials. It has been found that the solidification rate of the melted alloy greatly influences the electrode performance, but views on the effect of the solidification rate on the electrode performance have differed [4–8]. In our previous work [8], the influence of the solidification rate on the performance of the alloy with composition $\text{MLNi}_{3.8}\text{Co}_{0.6}\text{Mn}_{0.55}\text{Ti}_{0.05}$ (ML denotes lanthanum-rich misch metal) has been investigated. Compared with casting, rapid quenching has produced alloys with longer cycle life. On the other hand, rapid quenching decreases the discharge voltage and capacity. The aim of this work is to investigate the dependence of the effect of the solidification rate on the composition, and hence the electrochemical properties, of AB_5 -type alloys.

^{*} Corresponding author.

2. Experimental

2.1. Alloy preparation

A master alloy of composition $\text{MmNi}_{3.6}\text{Co}_{0.75}\text{Mn}_{0.55}\text{Al}_{0.1}$ (where Mm denotes Ce-rich Mishmetal with purity of 99.5%, which comprises of 46 wt.% Ce, 27 wt.% La, 21 wt.% Nd, 5.6 wt.% Pr and 0.5 wt.% impurity) was prepared by induction melting of the commercial metals Mm, Ni, Co, Mn and Al (purity 99.9% for Ni, Co, Mn and Al). After induction melting, the melt was rapidly cooled by pouring into a copper mould which was cooled by water. Part of the cast alloy was re-melted and quenched by the melt-spinning method. Different quenching rates were adopted and are expressed by the linear velocities of the copper wheel used for the rapid quenching process.

2.2. Composition analysis

Various methods were employed to determine the composition of the test alloys. The gravimetric method was used for Mm (all rare earth elements as a whole), the dimethylglyoxime gravimetric method for Ni, the potentiometric titration method for Co, and the inductively coupled plasma-atomic emission spectrometry (ICP-AES) method for both Mn and Al.

2.3. Electrode preparation and electrochemical measurements

The fractions of both cast and quenched materials that passed a 250-mesh sieve were used for preparation of the electrodes. The electrode pellets (11 mm in diameter) were prepared by first mixing 0.5 g of hydride-forming alloy powder without so-called micro-encapsulations with fine nickel powder in a weight ratio of 1:2 together with a small amount of polyvinyl alcohol (PVA) solution as a binder, and then compressing the mixture at 3200 kg cm^{-2} after vacuum drying at 80°C for an hour. To prevent the electrode plate breaking into pieces with charge–discharge cycling, it was clamped and pressed against porous nickel. Before the experiments, the sample electrodes were immersed in the electrolyte for at least 1 day in order to wet fully the electrode.

The activation of the electrodes was completed by fully charging the pellets at a constant current density of 60 mA g^{-1} and, after a 20-min pause, by discharging at the same current density to -0.500 V with respect to a Hg/HgO reference electrode. This charge–discharge process was repeated for 10 cycles. The capacities and the discharge voltage (vs. Hg/HgO)–time curves at various discharge current densities, viz., 90, 120, 150, 240 and 300 mA g^{-1} were measured within 50 cycles. From the 50th cycle, two constant current densities, 300 mA g^{-1} and 60 mA g^{-1} (only once every 50 cycles for 60 mA g^{-1}), were em-

ployed for charging–discharging to measure the cycle durability. NiOOH plates and 6 M KOH solution were used as the counter-electrodes and the electrolyte, respectively. Each cycle was carried out by fully charging and discharging to -0.500 V with respect to a Hg/HgO reference electrode at the same temperature 25°C .

2.4. Phase and microstructure determination

The phase structure of the samples was determined by X-ray diffraction (XRD) analysis using an X-ray diffractometer with $\text{Co K}_{\alpha 1}$ radiation. The powder samples for the XRD measurement were coated with epoxy resin to protect the samples from oxidation during the measurement process.

The microstructure of the alloys before electrochemical cycling was investigated by using JEM-6400 scanning electron microscope (SEM) with energy dispersive analyzer of X-rays (EDAX).

3. Results and discussion

3.1. Results of composition analysis

All the alloys were analyzed with multiple methods described in Section 2. They were found to have almost

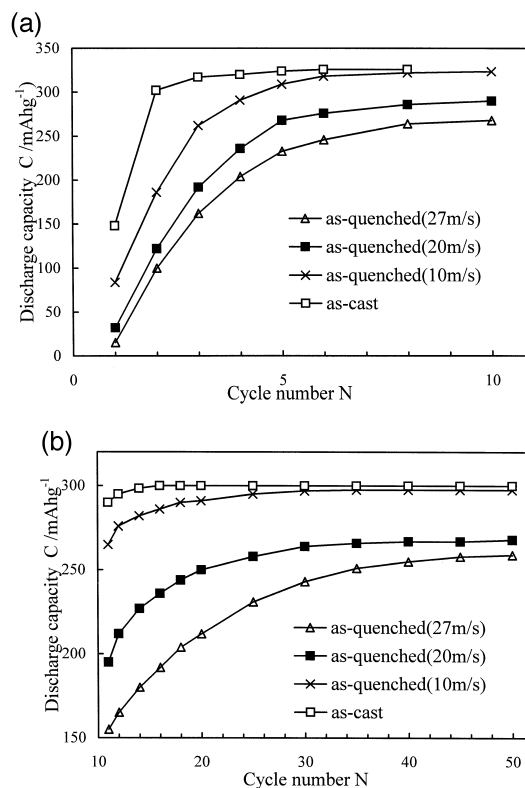


Fig. 1. Relationship between discharge capacity C and cycle number N over first 50 cycles with constant charge/discharge currents of (a) 60 mA g^{-1} and (b) 300 mA g^{-1} .

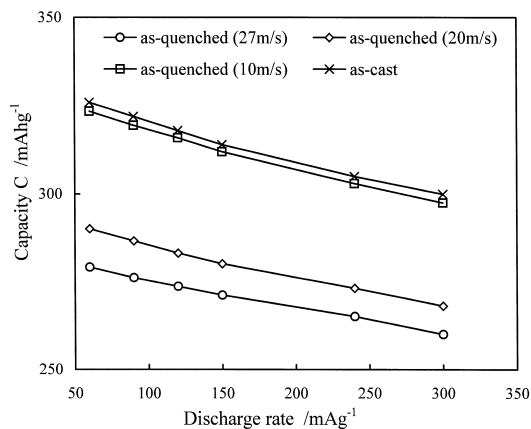


Fig. 2. Dependence of capacity on discharge rate at 25°C of cast alloy and rapidly quenched alloys with quenching rates of 10, 20 and 27 m s⁻¹, respectively.

the same composition before and after quenching. Thus, the observed changes in electrochemical properties and microstructures are not caused by composition changes.

3.2. Electrochemical measurements

3.2.1. Activation rate

As shown in Fig. 1, it is more difficult to activate completely the as-quenched alloy than the as-cast one. This finding differs from a previous observation [7] that the activation rate is greatly improved by rapid solidification with alloys of composition LaNi_{4.6}Al_{0.4} and LaNi₄Co_{0.6}Al_{0.4}. This suggests that the effect of rapid quenching on the activation rate of the AB₅-type hydrogen-storage alloys may vary with alloy composition. It has been shown [7] that grain boundaries can provide a good diffusion path for hydrogen for activating the electrode at a higher rate, and that the high-rate discharge capacity of the quenched alloy is larger than that of the cast one with the same composition because quenching produces smaller grains and many more boundaries. This conclusion does not agree with the above phenomena nor with the results of our previous work [8]. Clearly, the effect of grain volume and grain boundary intensity on the activation rate and the capacity requires further study and elucidation.

3.2.2. Dependence of capacity on discharge current

The dependence of discharge capacity on discharge current is shown in Fig. 2. In general, the discharge

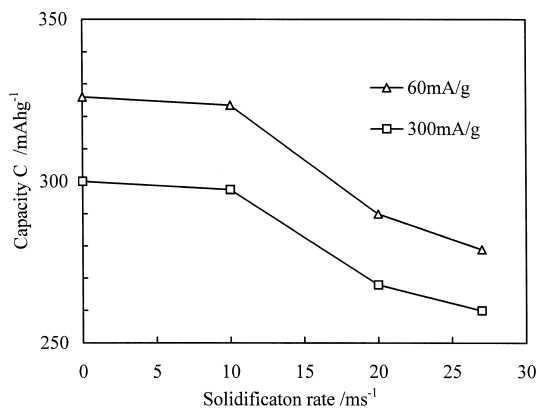


Fig. 3. Relationship between discharge capacity and solidification rate.

capacities of the rapidly quenched alloys are lower than that of the cast alloy. This differs from the results of other workers, namely, that the maximum capacities of the two kinds of electrodes are almost the same [6]. An amorphous phase and many more boundaries were produced by rapid quenching and this should account for the reduction of capacity. As shown in Fig. 3, both high (300 mA g⁻¹) and low (60 mA g⁻¹) rate discharge capacities decreased with increasing solidification rate. It has been found [9] that amorphous LaNi₅ absorbed less than half the amount of hydrogen taken up by crystalline LaNi₅. There is, however, very little effect of solidification rate on the rate capability (see Table 1).

3.2.3. Cycle stability

Despite the above disadvantages of the melt-spinning method, it is found that all the quenched alloys have much better long-term cycle characteristics than the master alloy (Table 2). The cycle durability increases with quenching rate. The reason for the prolonged cycle life is that the pulverization of the alloys due to cycling can be suppressed because the volume changes induced by hydrogen charge–discharge cycles are lessened by the smaller grain size. It is well known metallurgically that a high solidification rate can prevent alloy crystals from growing too large, i.e., the higher the quenching rate, the smaller the grains. SEM observations reveal that the grain size of the quenched alloy with a quenching rate of 20 m s⁻¹ is below 1 μm,

Table 1

Relative capacities at different discharge currents (mA g⁻¹) (taking capacity at a discharge rate of 60 mA g⁻¹ as 100)

Sample	Relative capacities at different discharge currents					
	60	90	120	150	240	300
As-quenched (27 m s ⁻¹)	100	98.92	98.03	97.13	94.98	93.19
As-quenched (20 m s ⁻¹)	100	98.79	97.59	96.55	94.14	92.41
As-quenched (10 m s ⁻¹)	100	98.76	97.68	96.44	93.66	91.96
As-cast	100	98.77	97.55	96.32	93.56	92.02

Table 2

Comparison of capacity decay rate (C_{\max} and C_{550} denote the maximum capacity and the capacity with cycle number of 550 at a certain discharge current, respectively)

Discharge current	Sample	C_{\max}	C_{550}	$(C_{\max} - C_{550})/C_{\max} \times 100\%$
60 mA g^{-1}	as-cast	326	265	18.7
	as-quenched (10 m s^{-1})	323	299	7.4
	as-quenched (20 m s^{-1})	290	271	6.7
	as-quenched (27 m s^{-1})	279	261	6.3
300 mA g^{-1}	as-cast	300	249	16.9
	as-quenched (10 m s^{-1})	298	277	7.0
	as-quenched (20 m s^{-1})	268	251	6.4
	as-quenched (27 m s^{-1})	260	244	6.1

but is greater than $50 \mu\text{m}$ for as-cast alloy. Compared with our early work [8], the stability improvement range might vary with alloy composition, which means that a high quenching rate is much more effective in improving the cycle durability for certain alloys than for others.

3.2.4. Discharge voltage characteristics

The as-quenched alloys have similar discharge characteristics to those of the as-cast alloy (Fig. 4). The discharge voltage vs. time curves were measured by fully charging the electrodes at 60 mA g^{-1} for 6 h and, after a 20-min pause, discharging at 60 mA g^{-1} to -0.500 V vs. a Hg/HgO reference electrode. As shown in Fig. 4, the higher the quenching rate, the flatter and higher the discharge plateau. Nevertheless, a comparison with previous results [8] suggests that the effect of the solidification rate on the height of the discharge plateau may vary with alloy composition.

3.3. Comparison of phase structure

XRD patterns for both the master and rapid-quenched materials are shown in Fig. 5. All alloys in the as-quenched state with different quenching rates display virtually identi-

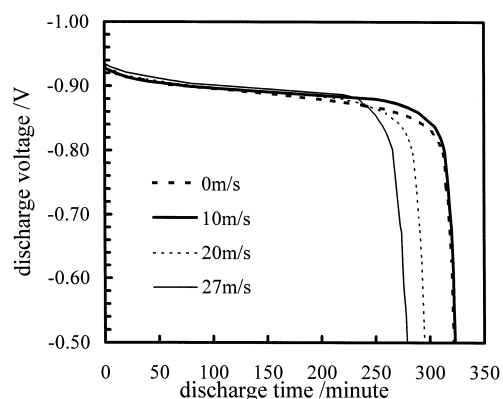


Fig. 4. Discharge voltage characteristics (discharge rate of 60 mA g^{-1}) of as-cast and as-quenched alloys.

cal pattern, except for small differences in intensity. Accordingly, only one X-ray pattern, for an alloy with a quenching rate of 27 m s^{-1} , is presented. At first glance, it can be seen from the diffraction patterns that in both materials the primary phase is the AB_5 compound (corresponding peaks have been indexed in Fig. 5). Despite this, striking differences in diffraction patterns can also be observed. First, for the rapidly quenched material, the well-defined diffraction peaks can be easily indexed to a AB_5 structure, while for the master alloy two diffraction peaks are encountered which cannot be easily indexed at 2θ angles of 36.5 and 37.9° . The two peaks are weak in intensity and this indicates a small quantity of segregation. Second, it is noticeable that the peaks the dominant phase for the two materials display different intensities and widths. For example, the peaks of the (111) and (200) planes are so wide that they overlap in the cast alloy, whereas they are discrete in the quenched alloy. All the

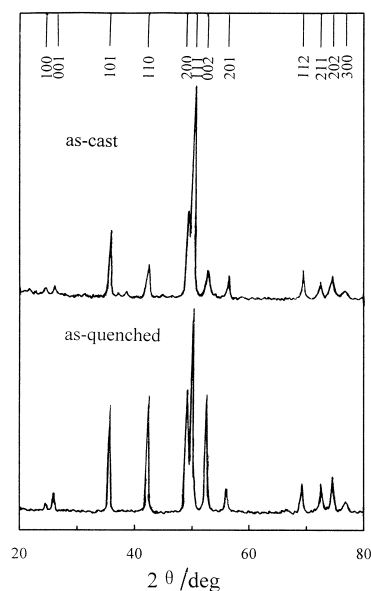


Fig. 5. X-ray diffraction patterns of master and the rapidly quenched (27 m s^{-1}) alloys (peaks indexed belong to AB_5 -type phase).

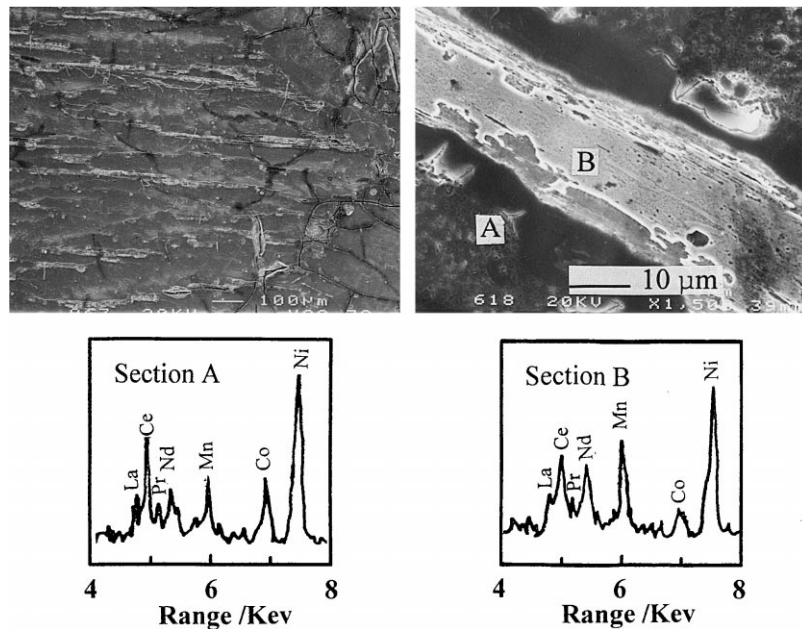


Fig. 6. Secondary electron micrographs of master alloy together with two typical EDAX spectra of sections A and B.

above phenomena should be taken as an indication that the master alloys are more inhomogeneous in composition and have more atomic disorder. Segregations are found in as-cast alloys by SEM observations (Fig. 6), while there are none in as-quenched alloys. This multi-phase microstructure could make the master alloy degrade rapidly during electrochemical cycling because different phases have different hardnesses and expansion coefficients, which lead to much larger mechanical stresses within the crystal

when absorbing/releasing hydrogen. By contrast, the quenched alloys have excellent cycle stability because they are very homogeneous in composition and had few second phases. Moreover, the improved cycle durability of the quenched alloys should be ascribed to the small grain size due to quenching (Fig. 7).

Further investigations, such as heat treatment and adjustment of composition, to obtain the best alloy are required. It has been reported that heat treatment can increase the capacity [10,11]. The new method needs special alloy compositions that are different from those of the conventional method. Practical AB_5 -type alloys usually introduce Co substitution for part of Ni. Cobalt is added mainly to achieve longer life, but it also causes a decrease in capacity, especially when measured at high discharge rates. As a result of the rapid quenching method, the Co content can be reduced, which should give an alloy with a large capacity at either low or high discharge rates, as well as long cycle life and lower cost.

4. Conclusions

Hydrogen-storage alloys with the composition $MmNi_{3.6}Co_{0.75}Mn_{0.55}Al_{0.1}$ have been investigated. Compared with casting, rapid quenching has produced alloys with different characteristics. The advantages are: (i) the long-term stability of the rapidly quenched materials is better than that of the conventionally prepared materials of the same composition; (ii) quenching flattens and raises the discharge plateau region to a more promising level. On the other hand, rapid quenching leads to a small decrease in capacity and slows down the activation of the electrode. The cycle durability increases and the capacity decreases

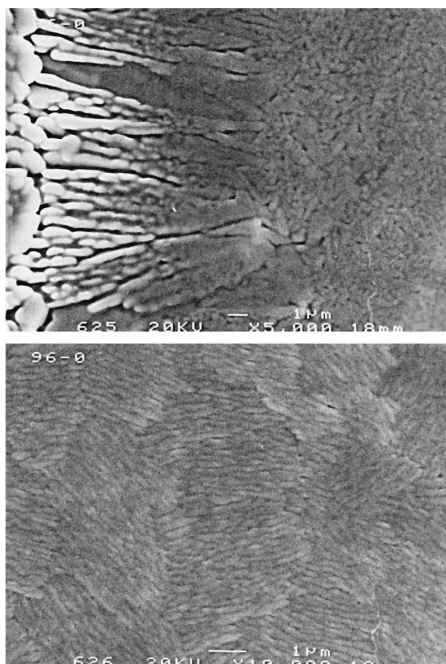


Fig. 7. Representative scanning electron images of quenched alloy (20 m s^{-1}): (a) cross section; (b) free surface of the flakes.

with increasing quenching rate. Thus, an optimum quenching rate should be chosen to maintain a balance between capacity and durability. Casting and rapid quenching produce different phase structures. Furthermore, the effect of the solidification rate on the performance of the AB₅-type alloys varies with alloy composition. Thus, a special composition should be selected to capitalize on the advantages of the high solidification techniques such as melt-spinning.

References

- [1] E.W. Justi, H.H. Eve, A.W. Kalberlah, N.M. Saridakis, M.H. Schaefer, *Energy Convers.* 10 (1970) 183.
- [2] J.J.G. Willems, *Phillips J. Res.* 39 (1984) 1, Suppl. 1.
- [3] P.H.L. Notten, P. Hokkeling, *J. Electrochem. Soc.* 138 (1991) 1877.
- [4] T. Sakai, H. Yoshinaga, H. Miyamura, N. Kuriyama, H. Ishikawa, *J. Alloys Comp.* 180 (1992) 37.
- [5] T. Sakai, T. Hazama, H. Miyamura, N. Kuriyama, A. Kato, H. Ishikawa, *J. Less-Common Met.* 172–174 (1991) 1175.
- [6] T. Weizhong, S. Guangfei, *J. Alloys Comp.* 203 (1994) 195.
- [7] R. Mishima, H. Miyamura, T. Sakai, N. Kuriyama, H. Ishikawa, I. Uehara, *J. Alloys Comp.* 192 (1993) 176.
- [8] C.-J. Li, X.-L. Wang, X.-M. Li, C.-Y. Wang, *Acta Metall. Sinica* 34 (1998) 288, (in Chinese).
- [9] H. Sakaguchi, T. Suemobu, K. Moriuchi, M. Yamagami, T. Yamaguchi, G.-Y. Adachi, *J. Alloys Comp.* 221 (1995) 212.
- [10] C.-J. Li, X.-L. Wang, J.-M. Wu, C.-Y. Wang, *J. Power Sources* 70 (1998) 106–109.
- [11] Y. Nakamura, H. Nakamura, S. Fujitani, I. Yonezu, *J. Alloys Comp.* 210 (1994) 299.